Published in final edited form as:
J Med Primatol. 2011 October ; 40(5): 300–309. doi:10.1111/j.1600-0684.2011.00475.x.

CD8+ Lymphocyte Depletion without SIV Infection does not Produce Metabolic Changes or Pathological Abnormalities in the Rhesus Macaque Brain

Eva-Maria Ratai[1,2], **Sarah Pilkenton**[1,2,&], **Julian He**[1,2], **Robert Fell**[1], **Jeffrey P. Bombardier**[1], **Chan-Gyu Joo**[1,2], **Margaret R. Lentz**[1,2], **Woong-Ki Kim**[3,*], **Tricia H. Burdo**[3,4], **Patrick Autissier**[3,4], **Lakshmanan Annamalai**[2,5,#], **Elizabeth Curran**[2,5], **Shawn O'Neil**[2,5,$], **Susan V. Westmoreland**[2,5], **Kenneth. C. Williams**[3,4], **Eliezer Masliah**[6], and **R. Gilberto González**[1,2]

[1]Department of Radiology, Neuroradiology Division and Athinoula A. Martinos Center for Biomedical Imaging, Massachusetts General Hospital, Charlestown, Massachusetts, 02129, USA

[2]Harvard Medical School, Boston, MA, 02115 USA

[3]Division of Viral Pathogenesis, Beth Israel Deaconess Medical Center, Boston, MA, USA

[4]Biology Department, Boston College, Chestnut Hill, MA, USA

[5]New England Primate Research Center, Southborough, Massachusetts, 01772, USA

[6]Department of Neurosciences, University of California at San Diego, La Jolla, CA, USA

Abstract

Background—Simian immunodeficiency virus (SIV) infection and persistent CD8+ lymphocyte depletion rapidly leads to encephalitis and neuronal injury. The objective of this study is to confirm that CD8-depletion alone does not affect brain pathology in the absence of SIV infection.

Methods—Four rhesus macaques were monitored by proton magnetic resonance spectroscopy (^{1}H-MRS) before and biweekly after anti-CD8 antibody treatment for eight weeks and compared to four SIV-infected animals. *Postmortem* immunohistochemistry was performed on these eight animals and compared to six uninfected, non-CD8-depleted controls.

Results—CD8-depleted animals showed stable metabolite levels and revealed no neuronal injury, astrogliosis or microglial activation in contrast to SIV-infected animals.

Conclusions—Alterations observed in MRS and lesions in this accelerated model of neuroAIDS result from unrestricted viral expansion in the setting of immunodeficiency rather than from CD8+ lymphocyte depletion alone.

Keywords

Magnetic resonance spectroscopy (MRS); NeuroAIDS; Accelerated SIV macaque model

Corresponding Author: R. Gilberto González, Neuroradiology Division, GRB 285, Massachusetts General Hospital, 55 Fruit St., Boston, MA 02114, Phone: (617) 726-8628, Fax: (617) 724-3338, rggonzalez@partners.org.
[&]Current address: Framingham State College, Framingham, MA
[*]Current address: Virginia Medical School, Norfolk, VA
[#]Current address: Oregon National Primate Research Center, Beaverton, OR
[$]Current address: Pfizer Inc., Chesterfield, MO

Introduction

Despite the effectiveness of highly active antiretroviral therapies (HAART), neurological complications of HIV infection (neuroAIDS) continue to be an important problem [4, 19, 28]. The simian immunodeficiency virus (SIV) is the closest known relative to HIV, and like HIV, productively infects CD4+ lymphocytes and monocyte/macrophage-derived cells including microglia, the resident macrophage of the brain [15, 37]. Similar to HIV patients who develop encephalitis, rhesus macaques infected with pathogenic strains of SIV such as SIVmac251 are susceptible to developing SIV encephalitis, the hallmarks of which include accumulation of viral-laden perivascular macrophages and multinucleated giant cells (MNGC), astrogliosis, microgliosis, and neuronal injury [6, 34].

However, the traditional SIV macaque model is limited in the sense that SIV encephalitis (SIVE) occurs in less than one-third of infected animals, and progression to terminal AIDS requires a lengthy time course of two or more years [7, 33]. Thus, attention has become focused on two rapidly progressing SIV macaque models. One model employs pigtailed macaques co-inoculated with immunosuppressive and neurovirulent viruses [36]. The second model retains the use of the SIV-infected rhesus macaque, but uses a monoclonal antibody to deplete the animal of CD8+ lymphocytes [29, 30]. In this model, more than 90% of persistently CD8-depleted animals develop histopathological signs of SIVE similar to those of HIV encephalitis [34]. Furthermore, using this accelerated model, we have demonstrated our ability to manipulate the severity of this damage, using a regimen of antiretroviral therapy [35] and minocycline [26]. However, in order to substantiate this animal model it is of vital importance to confirm that CD8 depletion alone does not result in astrogliosis and neurodegeneration.

Proton magnetic resonance spectroscopy (^{1}H MRS) is one of the most informative methods employed in neuroAIDS research [3, 5, 20]. ^{1}H MRS can non-invasively measure a wide range of cerebral metabolites *in vivo*, including the neuronal marker N-acetylaspartate (NAA) [21, 32] and putative glial markers of choline-containing metabolites, collectively abbreviated as Cho and *myo*-inositol (MI). Previously, our group has shown that SIV infection and CD8 depletion result in a rapid decline in NAA/Cr, indicative of MRS-detectable neuronal injury. [26, 35] Furthermore, Cho and MI are elevated with SIV infection [10, 27]. To confirm *in vivo* MRS results, we conducted quantitative immunohistochemistry (IHC) for the neuronal markers microtubule-associated protein (MAP2) and synaptophysin (SYN), astroglial marker glial fibrillary acidic protein (GFAP), and micriglial marker ionized calcium binding adaptor molecule 1 (IBA-1).

Materials and Methods

Non-Human Primates

A total of fourteen rhesus macaques (*Macaca mulatta*) were used in this study. All animals were housed according to the standards of the American Association for Accreditation of Laboratory Animal Care, and all investigators adhered to the Guide for the Care and Use of Laboratory Animals of the Institute of Laboratory Animal Resources, National Research Council. The study was approved by the Massachusetts General Hospital Subcommittee on Research Animal Care as well as the Institutional Animal Care and Use Committee of Harvard University. All animals were housed at the New England Primate Research Center (NEPRC) and animals were transported to the Center for Comparative Medicine (CCM) at the Massachusetts General Hospital for the 2 month duration of the imaging studies.

All animals were confirmed serologically negative for SIV, Simian T-Cell Leukemia Virus (STLV), and simian type D retrovirus (SRV) prior to initiation of study. Four of the fourteen

rhesus macaques were CD8+ lymphocyte-depleted by treatment with anti-CD8 antibody (cM-T807) administered once subcutaneous (s.c.) (10 mg/kg) and then intravenous (i.v.) (5 mg/kg) 2 and 4 days later. Animals in this group were not infected with SIV. To investigate potential metabolic changes, we performed MR spectroscopy on these animals before and biweekly following CD8 depletion, until 8 weeks post-depletion (w.p.d.). CD8-depleted animals were evaluated over a similar time course as SIV-infected, CD8-depleted animals allowing comparable end stage time points [26, 35].

For pathology studies, we performed retrospective analyses of two additional cohorts. Six animals were neither SIV-infected nor CD8-depleted and served as controls in this study. Four animals were inoculated intravenously with the simian immunodeficiency virus SIVmac251 (20 ng SIVp27, i.v.) and CD8+ T-lymphocyte depleted by treatment with anti-CD8 antibody (cM-T807) administered s.c. (10 mg/kg) 6 days post-infection and i.v. (5 mg/kg) 8 and 12 days post-infection (d.p.i.). SIV-infected, CD8-depleted animals were sacrificed between 8 and 12 weeks post infection. MRS and pathology findings of these four macaques were previously described in a paper by Williams et al. [35]. Table 1 summarizes the study.

MRI and MRS

We acquired *in vivo* MRS on the four CD8-depleted rhesus macaques using an 18 cm-diameter TEM transmit-receive coil (MR Instruments, Minneapolis, MN) on a 7T MRI scanner (Siemens AG, Erlangen, Germany). First, we employed a three-plane localizer to position the monkey in the coil; in this manner, voxel placement was highly reproducible. To image-guide the ^{1}H MRS volume of interest (VOI), we obtained sagittal, coronal and axial turbo spin echo [TE/TR=13/5000 ms, 160° flip angle, 160×160 mm^2 field-of-view (FOV), 512×512 matrix, and 2 mm slice thickness] images. The axial images were aligned parallel to the genu-splenium line of the corpus callosum on the sagittal projection.

Single voxel ^{1}H MR spectra from the white matter semiovale (WM), frontal cortex at the midline (FC), and the basal ganglia (BG) were acquired using a point-resolved spectroscopy (PRESS) sequence [TE/TR = 30/2500 ms and 192 acquisitions, bandwidth 1200 Hz] with WET water suppression (water suppression enhanced through T1 effects). Metabolite concentrations of NAA, Cho, MI, creatine (Cr), and glutamine and glutamate (Glx) were quantified using the LCModel software package (Stephen Provencher, Canada) [24] as ratios over Cr and using the unsuppressed water peak as reference. We generated the basis set or model functions to analyze the metabolites via LCModel using GAMMA software (ETH Zürich), a program designed to simulate magnetic resonance spin systems with the prior knowledge of all chemicals shifts and coupling constants for metabolites.

Flow Cytometry

Flow cytometry was used to monitor CD8+ lymphocyte depletion prior to antibody treatment and after CD8-depletion treatment, weekly thereafter. Flow cytometric analyses were performed with 100-μl aliquots of blood incubated with fluorochrome-conjugated antibodies including anti–CD3-APC (clone FN18; BioSource International, Camarillo, CA), anti–CD4-FITC (OKT4; Ortho Diagnostic Systems, Raritan, NJ), anti–CD8-PE (DK25; DakoCytomation, Glostrup, Denmark), and anti–CD20–PE–Texas Red (B1; Beckman Coulter, Brea, CA). Following antibody incubation at room temperature for 15 minutes, cells were washed twice with PBS containing 2% FBS, lysed the erythrocytes using the ImmunoPrep Reagent System (Beckman Coulter, Brea, CA), and washed the samples with PBS; after resuspending them in 2% formaldehyde in PBS, we analyzed the samples on a FACSCalibur flow cytometer (BD). Absolute numbers of CD8+ and CD4+ lymphocytes were determined by multiplying the percentage of CD8+/CD3+ or CD4+/CD3+ T cells by

absolute lymphocyte counts obtained using a standard veterinary 3-point WBC differential, CBC Hematology Analyzer (Hema-True, HESKA, Loveland, CO).

Tissue collection and processing

On the day of sacrifice, all animals were anesthetized with ketamine-HCl and euthanized by intravenous pentobarbital overdose. Animals were perfused with 4 liters of chilled saline. A complete set of CNS and peripheral tissues were collected in 10% neutral buffered formalin, embedded in paraffin, and sectioned at 6 μm. CNS histopathology with routine H&E slides was conducted on 10 different brain regions (prefrontal cortex, frontal cortex, parietal cortex, basal ganglia, amygdala, thalamus, hippocampus, cerebellum, brain stem, and cevial spinal cord.

Immunohistochemistry

Immunohistochemistry (IHC) was used to analyze the prevelance of CD8+ cells in the brain of the animals in the study using an antibody directed against CD8 (clone 1A5, 1:50, IgG1, Vector Labs). IHC was performed on 5 μM sections of formalin-fixed, paraffin-embedded (FFPE) tissues, using an ABC immunoperoxidase technique as described elsewhere [1]. Briefly, FFPE tissue sections were deparaffinized in xylene and rehydrated through graded ethanol to distilled water. Antigen retrieval was accomplished using a pressure cooker and Trilogy solution (Cell Marque, Rocklin, CA). Endogenous peroxidase activity was blocked in 3% hydrogen peroxide in phosphate buffered saline (PBS), and non-specific protein binding was blocked with Protein Block (Dako). After incubating with the primary antibody, tissue sections were reacted sequentially with biotinylated secondary antibody (Dako), horseradish peroxidase-conjugated streptavidin (Dako), and the chromogenic substrate 3, 3′-diaminobenzidene (DAB, Dako), and counterstained with hematoxylin (Sigma Chemical Co., St. Louis, MO). Objective scoring of brain sections was accomplished by examining at least 20 non-overlapping fields at 10× magnification and counting CD8+ DAB stained cells within either the meninges or parenchyma. The scoring system was as follows: 0 = no immunopositive cells observed in the section; + = rare scattered immunopositive cells within the entire section; ++ = 1-2 immunopostitive cells per 10× field.

Brain tissue from the frontal cortex was harvested in blocks, fixed in 10% neutral-buffered formalin, embedded in paraffin, and sectioned at 5μm for routine histology and quantitative neuropathology. The degree of reactive astrogliosis was assessed with monoclonal anti-glial fibrillary acidic protein (1:1000; Boehringer Mannheim, Indianapolis, IN). 5 μm-thick paraffin sections from the frontal cortex were immunolabeled overnight with these monoclonal antibodies, followed by biotinylated horse anti-mouse immunoglobulin G, avidin-horseradish peroxidase (Vectastain Elite kit; Vector, Burlingame, CA), and reacted with diaminobenzidine tetrahydrochloride and peroxide (0.03%). We evaluated the integrity of the synapses with monoclonal antibody against synaptophysin (1:10) (Boehringer Mannheim, Indianapolis, IN), and evaluated the status of neuronal dendrites using monoclonal antibody against microtubule-associated protein 2 (MAP2) (Boehringer Mannheim, Indianapolis, IN).

Levels of GFAP, synaptophysin, and MAP2 were determined by way of computer-aided image analysis, as previously described [18]. Immunoreactivity was semiquantitatively assessed as corrected optical density, using a microdensitometer (Quantimet 570C; Leica, Microsystem Cambridge, UK). For this purpose, three immunolabeled sections from each case were analyzed. As previously described [13, 16, 18], the microdensitometer system was first calibrated with a set of filters of various densities, ten images for each section at ×100 magnification were obtained. After the area of interest (layers 2–5) was delineated with the cursor, the optical density within that area was obtained. The optical density in each image

was averaged and expressed as the mean per case. All of the measurements for MAP2 and synaptophysin are in arbitrary optical density units, and range from 0 to 500 (*i.e.*, 0 indicates all light is allowed to pass through the sample, while 500 indicates no light is allowed to pass through the sample). All values are expressed as mean ± standard error of the mean.

Microglial activation was assessed by quantifying calcium binding adaptor protein 1 (IBA-1) (Wako Corp. Japan). Images of tissue sections were captured without manipulation using an Olympus 3-CCD T60C color video camera mounted on an Olypus Vanox-SI microscope and analyzed using NIH Image J software.

Statistical Analysis

We performed repeated measures analysis of variance (RM ANOVA) and Holm's t-tests using JMP 7.0 (SAS, Cary, NC) to examine the metabolic changes by *in vivo* MRS. Analysis of variance (ANOVA) was used to determine the significance of changes for each neuropathological marker between the three cohorts. Least squares means t-tests were used to isolate specific significant changes between cohorts only if statistical significance was determined with ANOVA. ANOVA was also used to detect an age effect between the three cohorts; a P-value of less than 0.05 was considered statistically significant.

Results

Flow cytometry on uninfected CD8-depleted animals

Flow cytometric analysis of peripheral blood confirmed that three out of the four uninfected CD8-depleted animals were persistently CD8+ lymphocyte-depleted for a minimum of 28 days. We observed the absolute CD8+ lymphocytes return by 21 days post-depletion in only one animal. Treatment with anti-CD8 antibody cM-T807 results in a depletion of both, CD3+CD8+ cells as well as natural killer (NK) cells [23].

CD8+ lymphocyte depletion resulted in a dramatic induction of CD4+ cells proliferation. Increases in CD4+ cells could be observed in both, the SIV+/CD8- and the CD8- cohorts. Table 1 shows the final CD4 counts before sacrifice. These findings are consistent with previously published results by Okoye et al [23]. Thus, CD4 cell count cannot be used to define AIDS illness in this accelerated macaque model of neuroAIDS.

MR spectroscopy in uninfected CD8-depleted animals

Prior to his study, we had performed a power analyses to ensure that four animals are sufficient to demonstrate the lack of anti-CD8 treatment response. The power calculation for this project was derived from our previously published work with SIV+/CD8- macaques [35] and is based on NAA/Cr levels in the frontal cortex. Using 1H MRS at 1.5 T, we had observed substantial decreases in frontal cortex NAA/Cr in SIV-infected, CD8+ T cell depleted rhesus macaques. T-tests revealed a 20% decrease between the pre-infection scan and the final scan between 8 and 12 wpi in the four untreated animals that progressed to terminal AIDS and developed SIVE. We assume that the total standard deviation consists of the instrumental error combined with the error generated by the biological diversity of the animals. Based on stability tests on animals that were scanned three or more times in the 7.0 T Instrument, we were able to determine the coefficient of variance for the same animal to be 3.5%. Thus, using four animals we are able to identify a minimal detectable difference of 7% in the same animals between pre and post depletion with 80% power at a two-sided 5% significance level. On the other hand, changes in metabolites are typically on the order of 20% for NAA/Cr at 8 wpi and 20-40% of Cho/Cr at 2 wpi and 8 wpi in SIV-infected CD8-depleted animals and should therefore be detectable.

In vivo ^{1}H MR spectra were acquired from the frontal cortex (FC), basal ganglia (BG) and white matter semiovale (WM). Figure 1 depicts a representative spectrum acquired from an animal prior to CD8 depletion. ^{1}H MR spectra acquired with short echo time (TE=30ms) are characterized by resonances primarily arising from N-acetylaspartate and N-acetylaspartylglutamate (collectively referred to as NAA), choline-containing compounds (referred to as Cho), *myo*-Inositol (MI), creatine-containing compounds (referred to as Cr) and the glutamate and glutamine concentrations (so-called Glx).

Figure 2a shows the changes over time in the metabolic ratios of NAA, Cho, MI and glutamate and glutamine (Glu+Gln, Glx) to creatine in the white matter (WM) in one representative animal before and after CD8 depletion. Metabolites did not reveal alteration due to the CD8 antibody treatment. Figure 2b shows the mean NAA/Cr ratios in the WM, FC and BG of the four CD8-depleted animals as a function of time post-CD8 depletion. Again, we found no significant changes in any of the brain regions over time. In addition, in all three brain regions we examined, we evaluated the changes in Cho/Cr, MI/Cr and Glx/Cr as well as the metabolite concentrations of Glx, NAA, Cho, MI and Cr using the unsuppressed water peak as reference before and after CD8+ lymphocyte depletion; we found no statistically significant changes due to CD8 depletion (RM ANOVA $p > 0.05$).

Histopathology and Quantitative Immunohistochemistry on a) SIV-infected CD8-depleted animals, b) uninfected CD8-depleted animals, and c) uninfected non-CD8-depleted animals

Table 1 summarizes the clinical and histopathological findings for all 14 animals included in the *postmortem* evaluations. All four CD8-depleted showed no significant clinical abnormalities. At day of necropsy animals presented in normal body condition. Their mesentrical lymph nodes were mildly enlarged consistent with increased lymphocyte proliferation [23]. In addition there was a small focus of lymphocytes in the choroid plexus and in the meningitis in two of these animals, respectively. Histopathologic review of H&E slides of the four CD8 depleted, uninfected control animals confirmed the absence of significant alteration in the CNS. There was no evidence of opportunistic infections that would suggest persistent immunosuppression. Lymphoid hyperplasia was observed in three of the four CD8 depleted uninfected controls consistent with observations made by other investigators that expansion of CD4 memory cells may occur as a consequence of CD8 depletion [23]. None of the uninfected macaques exhibited immunosuppressive disease or CNS inflammation.

In contrast, all four of the animals that were infected intravenously with SIVmac251 and depleted of CD8+ lymphocytes developed AIDS and SIVE. AIDS was confirmed by the histopathologic presence of one or more of the following AIDS defining lesions: opportunistic infections, giant cell encephalitis, giant cell pneumonia, pulmonary arteriopathy, lymphoid depletion, or wasting [12, 14]. SIVE was defined by the presence of MNGC, accumulation of viral-laden perivascular macrophages and presence of virus in the brain.

In general, immunohistochemical detection of CD8+ lymphocytes in brain in all groups revealed rare to occasional CD8+ cells particularly within the meninges, around blood vessels, and rarely scattered within the parenchyma. Fewer cells were observed within the meninges and parenchyma of CD8-depleted uninfected animals compared to those of the non-depleted uninfected controls. Analysis of SIV-infected CD8-depleted animals revealed slightly higher presence of CD8+ cells particularly within the meninges, which may reflect newly infiltrating cells consistent with re-emergence of CD8+ cells within the peripheral circulation (Table1).

We quantified SYN, MAP2, and GFAP levels in the frontal cortex (FC) of eight SIV-infected CD8-depleted animals, the four uninfected, CD8-depleted animals and six uninfected non-CD8-depleted controls. Overall, neuronal/astroglial markers were not found to differ between the two uninfected control cohorts. However, infected animals revealed decreased levels of both SYN and MAP and increased levels of GFAP compared to the two control cohorts. Figure 3a illustrates the mean SYN levels of each cohort (ANOVA $p = 0.014$). We observed statistically significant differences between the SIV-infected CD8-depleted animals (SIV+/CD8-) and the uninfected non-CD8-depleted animals (controls) ($p = 0.0046$) as well as between the SIV+/CD8- macaques and the uninfected CD8-depleted animals (CD8-) ($p = 0.039$). More importantly, there was no statistically significant difference in SYN between CD8-depleted and non-depleted controls ($p = 0.35$). Figure 3b shows the mean MAP2 levels of each cohort. Though differences between the cohorts are not significant (ANOVA $p = 0.24$), infected SIV+/CD8- animals exhibited markedly lower MAP2 levels compared to both control cohorts, while CD8-depleted and non-depleted controls had approximately the same levels of MAP2.

GFAP measured in the frontal cortex (Figure 3c) revealed statistically significant differences between the cohorts ($p = 0.0002$). GFAP levels were significantly elevated in SIV+/CD8-animals compared to non-depleted controls ($p = 0.0001$) and to CD8-depleted animals ($p = 0.0002$). There was no statistically significant difference in GFAP between non-depleted controls and CD8-depleted animals ($p = 0.92$).

The extent of microglial activation was quantified using ionized calcium binding adaptor molecule-1 (IBA-1). Calcium binding adaptor protein 1, IBA-1 is expressed by resting microglia and is upregulated when these cells are activated [11]. Widespread microglial activation accompanied by intense staining of IBA-1 was observed in SIV+/CD8-animals euthanized 8-12 weeks post infection. IBA-1 measured in the frontal cortex (Figure 3d) revealed statistically significant differences between the cohorts ($p = 0.0003$). IBA-1 levels were significantly elevated in SIV+/CD8-animals when compared to non-depleted controls ($p = 0.0003$) and to CD8-depleted animals ($p = 0.0002$). There was no statistically significant difference in IBA-1 between non-depleted controls and CD8-depleted animals ($p = 0.88$).

Discussion

To our knowledge this is the first neuropathology and neuroimaging study to address whether CD8+ lymphocyte depletion without SIV infection affects brain metabolism and/or results in neuronal injury/astrogliosis. Our results demonstrate that none of the CD8-depleted uninfected macaques (n=4) developed symptoms of AIDS or SIVE, while all infected animals developed AIDS and SIVE (n=4). In the current study, we performed MRS to determine whether metabolic changes detected by MRS could be attributable to CD8 depletion. The noninvasive nature of *in vivo* MRS permits data acquisition at multiple time points, eliminating the need for serial sacrifice studies and minimizing the number of animals needed. Nevertheless, there are limitations to the quality of *in vivo* spectra, which are usually obtained at low field strengths. To improve the sensitivity in this study, we performed MRS on a high magnetic field (7 Tesla) scanner to ensure we could detect metabolic changes due to CD8 depletion, if they were present. It has been shown that higher field strengths yield better signal-to-noise ratio, higher spectral resolution, and therefore, improved quantification precision [8, 25, 31]. MRS revealed that neither NAA/Cr nor NAA changed significantly after treatment with anti-CD8 antibody. Similarly, glial markers Cho and MI did not show significant alteration upon CD8 depletion. The lack of observable deviations from baseline in metabolite levels indicates that CD8+ lymphocyte depletion does not significantly impact brain metabolism.

Previously, our group has shown that SIV infection and CD8 depletion result in a rapid decline in NAA/Cr; after eight weeks SIV infection and CD8 depletion, NAA/Cr levels were significantly lower compared to pre-infection values in all brain regions we examined [26, 35]. In the acute stage of SIV infection without CD8 depletion, we observed transient and reversible NAA/Cr changes in the frontal cortex [10], which led us to speculate that longitudinal analysis of NAA/Cr could be a marker of the dynamic processes involved in neuronal injury and repair. Additionally, we found that NAA/Cr correlated best with synaptophysin compared to MAP2 and neuronal density during this reversible neuronal injury in the early stages of disease [16]. Furthermore, NAA/Cr accurately corresponds to degree of CNS inflammation; specifically the magnitude of decrease in NAA/Cr ratio has been found to be associated with severity of SIVE [17]. Hence, NAA/Cr is believed to be a very sensitive, reliable marker of neuronal injury and dysfunction.

Typically, increases in Cho and MI are considered to reflect increases in glial activity [2]. In the SIV-infected CD8-depleted macaque model, we found a temporal increase in Cho and Cho/Cr at 2 weeks post infection (wpi), and a subsequent decrease to baseline and below 4 wpi, consistent with the acute phase of SIV infection [10, 27]. At later stages, 8 wpi, Cho and Cho/Cr increased once again, suggesting a second increase of gliosis. MI level appears to be elevated at 2 and 4 wpi, and subsequently decreases back to baseline levels [26].

In addition, we conducted histopathological examination to evaluate the pre-synaptic and dendritic integrity of tissue from the frontal cortex. Decreases in the expression of neuronal markers synaptophysin (SYN), an integral protein in presynaptic terminals, and microtubule-associated protein 2 (MAP2), a marker for neuronal cell bodies and dendrites, have been shown to reflect the severity of neurodegeneration [22]. Consistent with previous findings [26, 35], we observed significantly decreased levels of SYN in SIV-infected animals compared to the two uninfected cohorts. Synaptophysin and MAP2 expression in uninfected CD8-depleted animals and uninfected controls showed no statistically significant difference upon comparison, confirming our MRS findings that suggested CD8+ lymphocyte depletion alone does not have measureable effects on neuronal integrity. Glial fibrillary acidic protein (GFAP) is rapidly synthesized by astrocytes in response to neurologic insult, and therefore, serves as a reliable marker of astrogliosis. The GFAP levels measured in the SIV+/CD8- animals were significantly higher than those in the uninfected cohorts, suggesting that astrocytes in the SIV+/CD8- animals suffered an insult as a result of SIV infection and consequently underwent astrogliosis. These results are also consistent with our previous findings [9, 13]. On the other hand, we observed no significant variation in GFAP levels in the uninfected, CD8-depleted cohort compared to uninfected controls, suggesting that CD8+ lymphocyte depletion alone has no significant effect on astrocytic processes in the macaque brain. In addition, we have demonstrated that the CD8-depleted control animals did not show significant evidence of microgliosis based on ionized calcium binding adaptor molecule 1 (IBA-1) immunohistochemical analysis. Immunohistochemical detection of CD8+ lymphocytes in brain in all three cohorts revealed rare to occasional CD8+ cells.

In conclusion, MR spectroscopy revealed that metabolite concentrations and ratios do not change with anti-CD8 treatment. IHC revealed no changes in neuronal integrity as well as no astroglial response due solely to anti-CD8 treatment. These findings confirm the validity of this accelerated rhesus macaque model of neuroAIDS and also prove that despite viral manipulation of the immune system, brain metabolism is preserved.

Acknowledgments

We thank Drs. Joanne Morris, Elisabeth Moeller, and Michael Duggan, Ms. Shannon Luboyeski and Diane Raikowsky and staff from the Center of Comparative Medicine at Massachusetts General Hospital, as well as Dr. Angela Carville from the NERPC for animal veterinary care. We also like to thank Michael O'Connell for pathology support on this study. In addition, we would also like to thank Dr. Ronald Desrosier for providing us with the inoculum, SIVmac251, Drs. Mike Piatak and Jeffrey Lifson for viral load analyses (SAIC Frederick, Inc), and Dr. Keith Reimann for the depleting anti-CD8 (human recombinant, cM-807) antibody. Reagents used in these studies were provided by the NIH Nonhuman Primate Reagent Resource (R24 RR016001, N01 AI040101). We wish to thank Nichole Eusemann for editing this manuscript and Dr. Elkan F. Halpern for statistical support.

Supported by NIH grants R21NS059331 (EMR), R01NS050041 (RGG), R01NS040237 (KW), R01NS37654 (KW), R01MH62962 (EM), HNRC MH59754 (EM), HNRC MH62512 (EM), NIH-NS051129 (MRL), and RR00168 (NEPRC Base Grant). The Massachusetts General Hospital Athinoula A. Martinos Center for Biomedical Imaging is also supported by the National Center for Research Resources grant number P41RR14075.

References

1. Annamalai L, Westmoreland SV, Domingues HG, Walsh DG, Gonzalez RG, O'Neil SP. Myocarditis in CD8-depleted SIV-infected rhesus macaques after short-term dual therapy with nucleoside and nucleotide reverse transcriptase inhibitors. PLoS One. 2010; 5:e14429. [PubMed: 21203448]
2. Avison MJ, Nath A, Berger JR. Understanding pathogenesis and treatment of HIV dementia: a role for magnetic resonance? Trends Neurosci. 2002; 25:468–473. [PubMed: 12183208]
3. Barker PB, Lee RR, McArthur JC. AIDS dementia complex: evaluation with proton MR spectroscopic imaging. Radiology. 1995; 195:58–64. [PubMed: 7892496]
4. Brodt HR, Kamps BS, Gute P, Knupp B, Staszewski S, Helm EB. Changing incidence of AIDS-defining illnesses in the era of antiretroviral combination therapy. Aids. 1997; 11:1731–1738. [PubMed: 9386808]
5. Chang L, Ernst T, Leonido-Yee M, Walot I, Singer E. Cerebral metabolite abnormalities correlate with clinical severity of HIV-1 cognitive motor complex. Neurology. 1999; 52:100–108. [PubMed: 9921855]
6. Crews L, Lentz MR, Gonzalez RG, Fox HS, Masliah E. Neuronal injury in simian immunodeficiency virus and other animal models of neuroAIDS. J Neurovirol. 2008; 14:327–339. [PubMed: 18780234]
7. Fuller RA, Westmoreland SV, Ratai E, Greco JB, Kim JP, Lentz MR, He J, Sehgal PK, Masliah E, Halpern E, Lackner AA, Gonzalez RG. A prospective longitudinal in vivo 1H MR spectroscopy study of the SIV/macaque model of neuroAIDS. BMC Neurosci. 2004; 5:10. [PubMed: 15070430]
8. Gonen O, Liu S, Goelman G, Ratai EM, Pilkenton S, Lentz MR, Gonzalez RG. Proton MR spectroscopic imaging of rhesus macaque brain in vivo at 7T. Magn Reson Med. 2008; 59:692–699. [PubMed: 18302225]
9. Gonzalez RG, Cheng LL, Westmoreland SV, Sakaie KE, Becerra LR, Lee PL, Masliah E, Lackner AA. Early brain injury in the SIV-macaque model of AIDS. Aids. 2000; 14:2841–2849. [PubMed: 11153665]
10. Greco JB, Westmoreland SV, Ratai EM, Lentz MR, Sakaie K, He J, Sehgal PK, Masliah E, Lackner AA, Gonzalez RG. In vivo 1H MRS of brain injury and repair during acute SIV infection in the macaque model of neuroAIDS. Magn Reson Med. 2004; 51:1108–1114. [PubMed: 15170829]
11. Ito D, Imai Y, Ohsawa K, Nakajima K, Fukuuchi Y, Kohsaka S. Microglia-specific localisation of a novel calcium binding protein, Iba1. Brain Res Mol Brain Res. 1998; 57:1–9. [PubMed: 9630473]
12. Kestler H, Kodama T, Ringler D, Marthas M, Pedersen N, Lackner A, Regier D, Sehgal P, Daniel M, King N, et al. Induction of AIDS in rhesus monkeys by molecularly cloned simian immunodeficiency virus. Science. 1990; 248:1109–1112. [PubMed: 2160735]
13. Kim JP, Lentz MR, Westmoreland SV, Greco JB, Ratai EM, Halpern EF, Lackner AA, Masliah E, Gonzalez RG. Relationship between astrogliosis and 1H MRS measures of brain Cho/Cr and MI/Cr in a primate model. AJNR Am J Neuroradiol. 2005; 6:752–759. [PubMed: 15814917]

14. King NW, Hunt RD, Letvin NL. Histopathologic changes in macaques with an acquired immunodeficiency syndrome (AIDS). Am J Pathol. 1983; 113:382–388. [PubMed: 6316791]
15. Lackner AA, Smith MO, Munn RJ, Martfeld DJ, Gardner MB, Marx PA, Dandekar S. Localization of simian immunodeficiency virus in the central nervous system of rhesus monkeys. Am J Pathol. 1991; 139:609–621. [PubMed: 1716047]
16. Lentz MR, Kim JP, Westmoreland SV, Greco JB, Fuller RA, Ratai EM, He J, Sehgal PK, Halpern EF, Lackner AA, Masliah E, Gonzalez RG. Quantative neuropathological correlates of changes in macque brain NAA/Cr. Radiology. 2005; 235:461–468. [PubMed: 15798152]
17. Lentz MR, Lee V, Westmoreland SV, Ratai EM, Halpern EF, Gonzalez RG. Factor analysis reveals differences in brain metabolism in macaques with SIV/AIDS and those with SIV-induced encephalitis. NMR Biomed. 2008; 21:878–887. [PubMed: 18574793]
18. Masliah E, Achim CL, Ge N, DeTeresa R, Terry RD, Wiley CA. Spectrum of human immunodeficiency virus-associated neocortical damage. Ann Neurol. 1992; 32:321–329. [PubMed: 1416802]
19. McArthur JC. HIV dementia: an evolving disease. J Neuroimmunol. 2004; 157:3–10. [PubMed: 15579274]
20. Meyerhoff DJ, MacKay S, Bachman L, Poole N, Dillon WP, Weiner MW, Fein G. Reduced brain N-acetylaspartate suggests neuronal loss in cognitively impaired human immunodeficiency virus-seropositive individuals: in vivo 1H magnetic resonance spectroscopic imaging. Neurology. 1993; 43:509–515. [PubMed: 8450992]
21. Moffett JR, Namboodiri MA, Cangro CB, Neale JH. Immunohistochemical localization of N-acetylaspartate in rat brain. Neuroreport. 1991; 2:131–134. [PubMed: 1768855]
22. Moore DJ, Masliah E, Rippeth JD, Gonzalez R, Carey CL, Cherner M, Ellis RJ, Achim CL, Marcotte TD, Heaton RK, Grant I. Cortical and subcortical neurodegeneration is associated with HIV neurocognitive impairment. Aids. 2006; 20:879–887. [PubMed: 16549972]
23. Okoye A, Park H, Rohankhedkar M, Coyne-Johnson L, Lum R, Walker JM, Planer SL, Legasse AW, Sylwester AW, Piatak M Jr, Lifson JD, Sodora DL, Villinger F, Axthelm MK, Schmitz JE, Picker LJ. Profound CD4+/CCR5+ T cell expansion is induced by CD8+ lymphocyte depletion but does not account for accelerated SIV pathogenesis. J Exp Med. 2009; 206:1575–1588. [PubMed: 19546246]
24. Provencher SW. Estimation of metabolite concentrations from localized in vivo proton NMR spectra. Magn Reson Med. 1993; 30:672–679. [PubMed: 8139448]
25. Ratai E, Kok T, Wiggins C, Wiggins G, Grant E, Gagoski B, O'Neill G, Adalsteinsson E, Eichler F. Seven-Tesla proton magnetic resonance spectroscopic imaging in adult X-linked adrenoleukodystrophy. Arch Neurol. 2008; 65:1488–1494. [PubMed: 19001168]
26. Ratai EM, Bombardier JP, Joo CG, Annamalai L, Burdo TH, Campbell J, Fell R, Hakimelahi R, He J, Autissier P, Lentz MR, Halpern EF, Masliah E, Williams KC, Westmoreland SV, Gonzalez RG. Proton magnetic resonance spectroscopy reveals neuroprotection by oral minocycline in a nonhuman primate model of accelerated NeuroAIDS. PLoS One. 2010; 5:e10523. [PubMed: 20479889]
27. Ratai EM, Pilkenton SJ, Greco JB, Lentz MR, Bombardier JP, Turk KW, He J, Joo CG, Lee V, Westmoreland S, Halpern E, Lackner AA, Gonzalez RG. In vivo proton magnetic resonance spectroscopy reveals region specific metabolic responses to SIV infection in the macaque brain. BMC Neurosci. 2009; 10:63. [PubMed: 19545432]
28. Sacktor N. The epidemiology of human immunodeficiency virus-associated neurological disease in the era of highly active antiretroviral therapy. J Neurovirol. 2002; 8 2:115–121. [PubMed: 12491162]
29. Schmitz JE, Kuroda MJ, Santra S, Sasseville VG, Simon MA, Lifton MA, Racz P, Tenner-Racz K, Dalesandro M, Scallon BJ, Ghrayeb J, Forman MA, Montefiori DC, Rieber EP, Letvin NL, Reimann KA. Control of viremia in simian immunodeficiency virus infection by CD8+ lymphocytes. Science. 1999; 283:857–860. [PubMed: 9933172]
30. Schmitz JE, Simon MA, Kuroda MJ, Lifton MA, Ollert MW, Vogel CW, Racz P, Tenner-Racz K, Scallon BJ, Dalesandro M, Ghrayeb J, Rieber EP, Sasseville VG, Reimann KA. A nonhuman

primate model for the selective elimination of CD8+ lymphocytes using a mouse-human chimeric monoclonal antibody. Am J Pathol. 1999; 154:1923–1932. [PubMed: 10362819]

31. Tkac I, Oz G, Adriany G, Ugurbil K, Gruetter R. In vivo 1H NMR spectroscopy of the human brain at high magnetic fields: metabolite quantification at 4T vs. 7T. Magn Reson Med. 2009; 62:868–879. [PubMed: 19591201]
32. Urenjak J, Williams SR, Gadian DG, Noble M. Specific expression of N-acetylaspartate in neurons, oligodendrocyte-type-2 astrocyte progenitors, and immature oligodendrocytes in vitro. J Neurochem. 1992; 59:55–61. [PubMed: 1613513]
33. Westmoreland SV, Halpern E, Lackner AA. Simian immunodeficiency virus encephalitis in rhesus macaques is associated with rapid disease progression. J Neurovirol. 1998; 4:260–268. [PubMed: 9639069]
34. Williams K, Alvarez X, Lackner AA. Central nervous system perivascular cells are immunoregulatory cells that connect the CNS with the peripheral immune system. Glia. 2001; 36:156–164. [PubMed: 11596124]
35. Williams K, Westmoreland S, Greco J, Ratai E, Lentz M, Kim WK, Fuller RA, Kim JP, Autissier P, Sehgal PK, Schinazi RF, Bischofberger N, Piatak M, Lifson JD, Masliah E, Gonzalez RG. Magnetic resonance spectroscopy reveals that activated monocytes contribute to neuronal injury in SIV neuroAIDS. J Clin Invest. 2005; 115:2534–2545. [PubMed: 16110325]
36. Zink MC, Clements JE. A novel simian immunodeficiency virus model that provides insight into mechanisms of human immunodeficiency virus central nervous system disease. J Neurovirol. 2002; 8 2:42–48. [PubMed: 12491150]
37. Zink MC, Spelman JP, Robinson RB, Clements JE. SIV infection of macaques--modeling the progression to AIDS dementia. J Neurovirol. 1998; 4:249–259. [PubMed: 9639068]

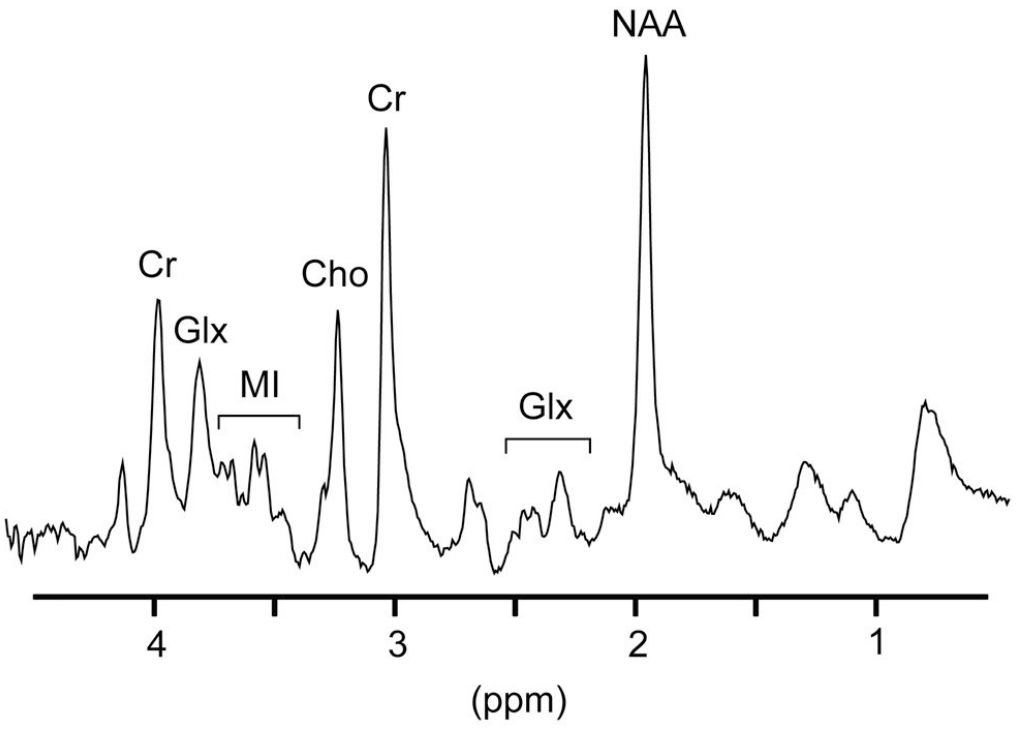

Figure 1.
Representative 7 Tesla MR spectrum acquired from the frontal cortex an animal prior to CD8 depletion. ^{1}H MR spectra are characterized by resonances primarily arising from N-acetylaspartate and N-acetylaspartylglutamate (collectively referred to as NAA), choline-containing compounds (referred to as Cho), *myo*-Inositol (MI), creatine-containing compounds (referred to as Cr) and the glutamate and glutamine concentrations (so-called Glx).

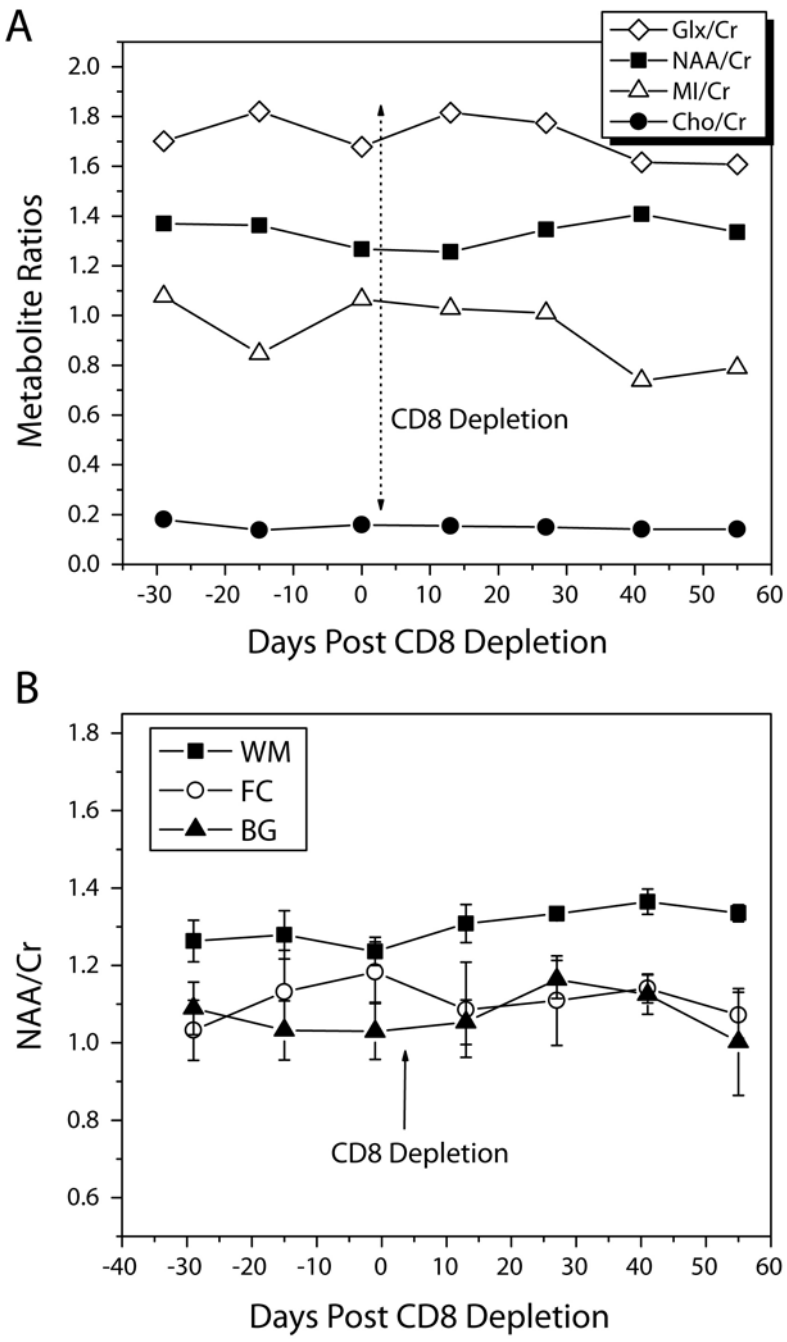

Figure 2.

Figure 2 (a). Changes in Glx/Cr, NAA/Cr, MI/Cr, and Cho/Cr in the white matter semiovale before and after CD8+ lymphocyte depletion in one representative animal over time. None of the metabolite ratios showed any change due to the anti-CD8 treatment.

Figure 2 (b). Mean NAA/Cr ratios of the four CD8-depleted animals in the white matter (WM), frontal cortex (FC), and basal ganglia (BG) as a function of time post-CD8 depletion. No significant changes in any of the brain regions over time were found.

The error bars represent standard error of the mean (SEM).

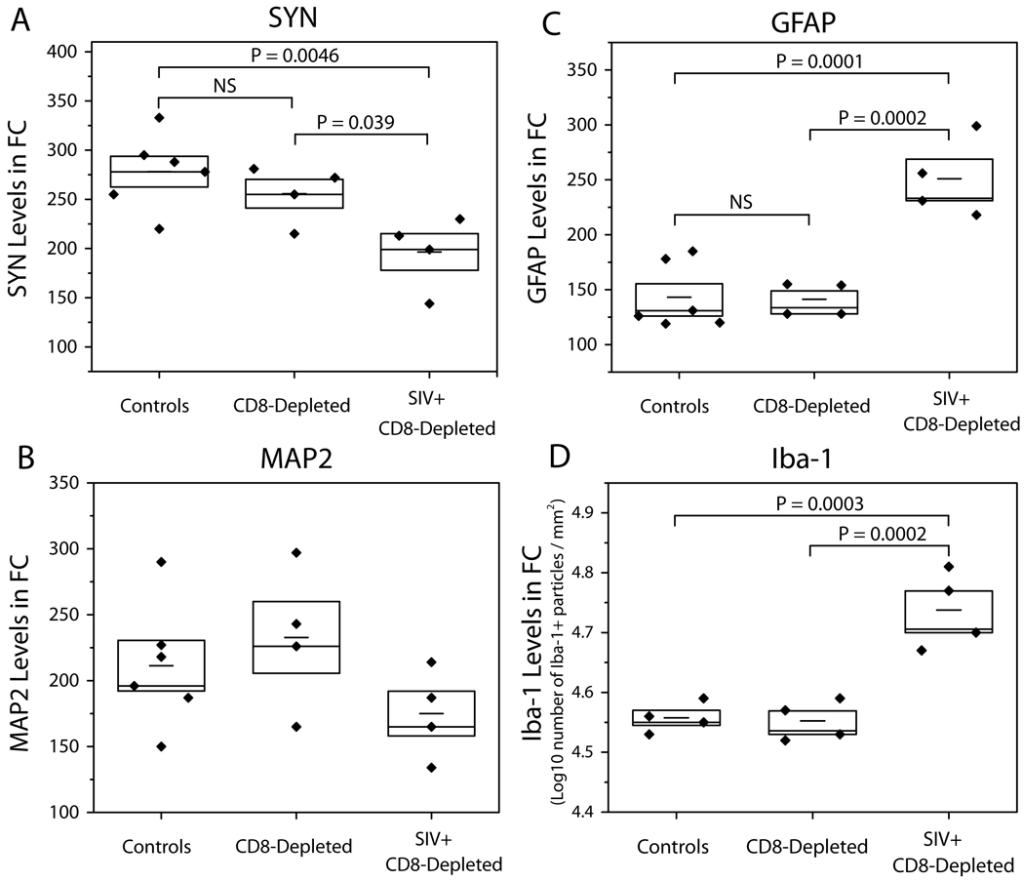

Figure 3.

Quantitative image analysis of immunohistochemistry reveals no difference between CD8-depleted, uninfected animals (CD8-) and non-CD8-depleted, uninfected controls (Control) in (**a**) SYN**,** (**b**) MAP2, (**c**) GFAP and **(d)** IBA-1; however, there are significant differences in SYN, GFAP and IBA-1 between SIV-infected, CD8-depleted animals (SIV+/CD8-) and these two control cohorts. Horizontal bars within boxes represent mean values; height of each box corresponds to standard error of the mean.

Table 1

Study summary

Animal	Study	Inoculated	CD8 depleted	AIDS	CNS Pathology	CD4+/CD3+ count at day of sacrifice	CD8 cells in the brain Scoring	
							meninges	parenchyma
A03-053	Ctrl 1	N	N	N	NSF	N.D.	++	+
A03-054	Ctrl 2	N	N	N	NSF	N.D.	++	++
A02-039	Ctrl 3	N	N	N	NSF	N.D.	+	+
A02-074	Ctrl 4	N	N	N	NSF	N.D.	0	+
A02-226	Ctrl 5	N	N	N	NSF	N.D.	0	+
A98-622	Ctrl 6	N	N	N	NSF	N.D.	N.D.	N.D.
A07-005	CD8- 1	N	Y	N	NSF	1720/μL	+	++
A07-006	CD8- 2	N	Y	N	NSF	1039/μL	0	0
A07-207	CD8- 3	N	Y	N	NSF	2193/μL	+	+
A07-208	CD8- 4	N	Y	N	NSF	770/μL	0	+
A02-712	SIV+/CD8- 1	Y	Y	Y	SIVE	1467/μL	++	++
A02-743	SIV+/CD8- 2	Y	Y	Y	SIVE	498/μL	++	+
A02-734	SIV+/CD8- 3	Y	Y	Y	SIVE	958/μL	++	+
A02-746	SIV+/CD8- 4	Y	Y	Y	SIVE	519/μL	0	+

NSF = no significant findings, N.D = Not determined.

CD8 + cells in the brain - scoring: 0 = no immunopositive cells observed in section; + = rare scattered cells;

Note that CD4 cells are artificially increased due to CD8-depletion and are therefore not useful for diagnosis of AIDS in the CD8-depleted macaque model of NeuroAIDS.